www.czasopisma.pan.pl PAN www.journals.pan.pl
POLSKA AKADEMIA NAUK

Arch. Min. Sci. **67** (2022), 3, 381-399

Electronic version (in color) of this paper is available: http://mining.archives.pl

DOI: https://doi.org/10.24425/ams.2022.142406

QIANG SUN[1*], CHENGFANG SHAN[2], ZHONGYA WU[1], YUNBO WANG[1]

CASE STUDY: MECHANISM AND EFFECT ANALYSIS OF PRESPLITTING BLASTING IN SHALLOW EXTRA-THICK COAL SEAM

The caving effect of the top coal caving is crucial for efficient mining. Using the Yushuling coal mine, Xinjiang province, China, as a case study, the coal and rock physical and mechanical parameters, such as the compressive, tensile, and shear strength values and hardness of the top coal and roof rock, were determined. The analysis of the effect of different factors on the blasting presplitting process was numerically simulated, and the optimal parameters of blast drilling were identified. Three presplit boreholes were implemented: in the workface, the workface's advance area, and the two roadway roofs in the workface's advance area. The optimal blasting drilling parameters and charge structure were designed. The field test results in the mine under study indicated that the top coal recovery rate of the 110501 fully mechanised top coal caving face was improved twice (from 40 to more than 80%), and an effective blasting presplitting was achieved. The proposed blasting presplitting method has an important guiding significance for fully mechanised top coal caving mining in Xinjiang and similar mining areas.

Keywords: Shallow-buried thick coal seam; hard roof and coal seam; fully mechanised top coal caving mining; blasting presplitting; parameter optimisation

1. Introduction

In recent years, with the large-scale, high-intensity, and continuous mining of coal resources, the shallow coal resources in developed areas of eastern China have become gradually exhausted. Meanwhile, the focus of the development of coal resources is being relocated to the Western area [1,2]. On the other hand, the distribution trend of coal resources in China can be described as "more in the West and North and less in the East and South." The western region contains about 80% of China's total coal resources, leading the area of their development and utilisation. The total amount of coal resources in the Xinjiang mining area is estimated to be about 2.2 trillion tons,

1 CHINA UNIVERSITY OF MINING AND TECHNOLOGY, CHINA
2 KUQA YUSHULING COAL MINE CO., LTD, KUQA, AKSU, CHINA
* Corresponding author: kkysun@126.com

© 2022. The Author(s). This is an open-access article distributed under the terms of the Creative Commons Attribution-NonCommercial License (CC BY-NC 4.0, https://creativecommons.org/licenses/by-nc/4.0/deed.en which permits the use, redistribution of the material in any medium or format, transforming and building upon the material, provided that the article is properly cited, the use is noncommercial, and no modifications or adaptations are made.

accounting for 40% of the country, ranking first. In 2020, the coal output in Xinjiang reached 250 million tons. With the rapid development of the national economy and society, the development of coal resources in Xinjiang plays an increasingly prominent role in China's power strategy [3,4].

Coal resources in Xinjiang mining areas are characterised by shallow burials and thick coal seams. In the mining process of coal resources, the mining face is affected by hard coal seam and hard roof, and the top coal caving is difficult (the average recovery rate is 30-40%), which seriously affects the mine production efficiency. At the same time, a large area of the hard roof is suspended during the mining, which increases the mine pressure and seriously affects its operation safety. At present, the top coal presplitting methods in fully mechanised top coal (FMTC) caving face, mainly includes blasting presplitting, hydraulic presplitting, carbon dioxide presplitting, etc. For example, based on the effect of FMTC caving in extra thickness coal seam with a hard dirt band by presplitting blasting, a cantilever beam model with non-uniform loading of dirt band's breaking was established [5]. The effects of horizon and thickness on the dirt band's breaking were also obtained. The hydraulic fracturing field tests to weaken the hard roof above the coal layer were conducted at the Coal Mine. The water pressure in boreholes and water seepage from bolt locations on two sides of roadways were monitored during hydraulic fracturing [6,7]. The hard roof's weakening effects versus the step size of periodic pressure, the dynamic loading factor, the roof's deflections, and the displacements of roadways were analysed. Zhang et al. [8] solved the technical problem of high-efficiency gas drainage in a deep low permeability coal seam, using the advantageous direction of jet fracturing under in-situ stress. It was based on theoretical analysis and novel technology for cracking and increasing permeability in a low-permeability coal seam. In particular, the LCO2 phase change directional jet fracturing was proposed and experimentally verified, with thickness varying from 166.10 m to 303.60 m. The above brief survey shows that the blasting presplitting technology is very mature, the presplitting effect is good, and the cracking is not affected by the in-situ stress [9], making it a widely used technology. However, this method is not universal for the mining quality characteristics of the Xinjiang mining area. It is necessary to further optimise the blasting presplitting method and process design.

Taking the Yushuling coal mine in Xinjiang as an example, this paper analyses the mining geological conditions of a shallow-buried double hard extra-thick coal seam and tests the physical and mechanical parameters of coal and rock samples in the workface area. It determines the key parameters of drilling and blasting, such as blasting hole diameter, hole spacing, decoupling coefficient, delay initiation time, etc., by the numerical simulation method [10,11]. Three kinds of roof blasting presplit boreholes (in the workface, in a coal seam in the workface's advance area, and two roadways in the workface's advance area) are optimised and designed. The synchronous presplitting of the main roof and coal seam is realised. The field application results show that this method can effectively improve top coal's caving rate in the top coal caving mining in shallow double hard and extra-thick coal seams. The application effect is remarkable, and the safe and efficient mining of coal resources is realised.

2. Mine overview

2.1. Mining geological conditions

Yushuling minefield is located at the southern foot of Tianshan Mountain. The terrain of the minefield is generally high in the north and the west and low in the south and the east.

The highest part of the minefield is located in the northwest of the minefield, with an altitude of 1907.77 m. The lowest part is located in the east of the minefield, with an altitude of 1743.80 m. The maximum elevation difference is 163.38 m, and the relative elevation difference is generally 10~50 m. The surface bedrock is exposed, and vegetation is scarce. The terrain in the north of the minefield is relatively flat. Most of the surface is covered by red burnt rock formed after spontaneous combustion of the coal seam. The gully is developed in some sections, and the terrain fluctuates considerably. The wind erosion landform composed of sandstone in the South is complex. The gullies in the area are mostly north-south.

At present, the Yushuling coal mine's production capacity is 1.2 million tons per year, the east-west direction of the mine is about 3.0 km long, the South-North width is approximately 3.3 km, and the area is about 9.3528 km^2. The geological structure in the minefield is simple, and the hydrogeological type is complex. At present, the normal water inflow of the mine is 88 m^3/h. At present, the first mining face is 110501, and the comprehensive mechanised top coal caving technology is adopted. The coal seam's average thickness is 8.6 m, the buried depth is about 100 m, the occurrence of the coal seam is stable, and there is no large structure. The immediate and main roofs are mainly fine sandstone and siltstone, with high compressive strength and hardness. The immediate roof is mainly siltstone, containing fine sandstone and coarse sandstone. The main roof is mainly grey-white siltstone, with fine sandstone and coarse sandstone, medium sandstone, and coarse gravel sandstone. Under dry and natural conditions, the main roof rock's compressive strength is relatively high, and it is not easy to deform. Under the saturated condition, the strength is greatly reduced. The saturated uniaxial compressive strength is 16.4~39.6 MPa. The natural uniaxial compressive strength is 28.4~61.0 MPa. The softening coefficient is 0.58~0.65, i.e., less than 0.75. The immediate floor is mainly fine sandstone with argillaceous siltstone, and its thickness range is between 1.41 and11.78 m. The main floor is mainly medium sandstone with coarse sandstone. Under the dry state, the rock's compressive strength with the direct bottom is relatively high, and it is not easy to deform. The 110501 workface layout and comprehensive histogram of regional boreholes are depicted in Fig. 1.

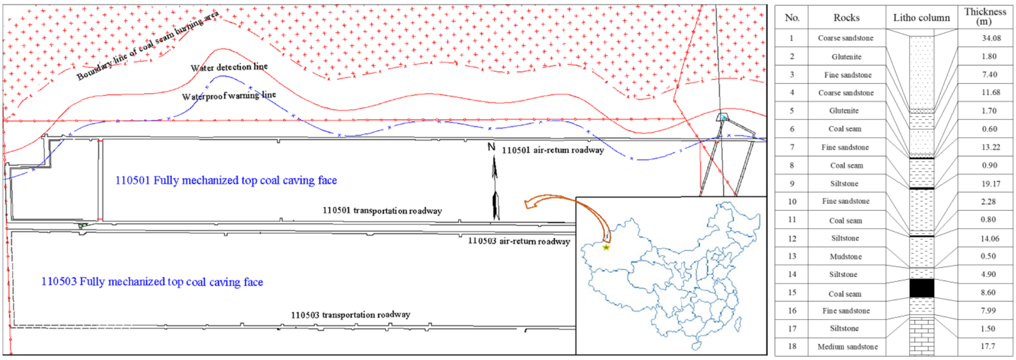

Fig. 1. The 110501 workface layout and comprehensive histogram of regional boreholes

2.2. Physical properties and mechanical characteristics of the coal seam and roof

The coal seam and roof's physical properties and mechanical characteristics were experimentally determined using coal and rock samples from the workface of the coal mine [12, 13]. The samples were extracted and processed via a ZS-100 vertical frequency conversion drilling sampler, SHM-200 double face grinder, and DQ-1 automatic rock cutting machine. A WAW-1000D microcomputer-controlled electro-hydraulic universal testing machine was used to carry out the following tests, and the load was implemented at a relatively slow rate (0.15-0.20 kN/s): (i) hardness test, (ii) uniaxial compressive strength test, (iii) tensile test, and (iv) rock sample variable-angle shear test, as shown in Fig. 2. The experimental results are listed in Tables 1-4.

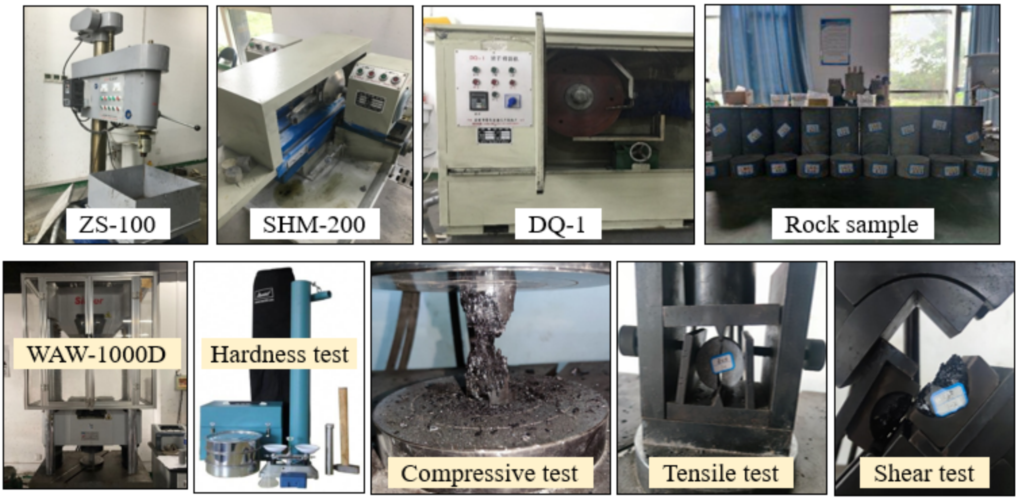

Fig. 2. Test process of physical and mechanical properties of coal and rock mass

TABLE 1

Uniaxial compressive strength results of coal and rock samples

Lithology	Diameter/mm	Height/mm	Failure load/kN	Uniaxial compressive strength s_c/MPa
Coal seam	49.7	102.7	44.43	22.91
	49.9	102.8	46.38	23.63
	49.8	102.7	44.97	22.64
Immediate roof	49.5	102.7	61.75	24.21
	49.8	103.0	68.93	27.03
	49.6	103.2	61.07	23.94
Main roof	49.7	102.7	113.60	44.54
	49.5	103.0	127.05	49.82
	49.8	103.2	114.02	44.71

TABLE 2

Splitting tensile test results of coal and rock samples

Lithology	Diameter/mm	Height/mm	Failure load/kN	Tensile strength s_t/MPa
Coal seam	49.7	25.6	1.87	0.95
	49.9	25.4	1.59	0.81
	49.8	24.8	1.12	0.57
Immediate roof	49.5	24.2	4.32	1.61
	49.7	25.1	2.66	0.99
	49.6	24.4	4.11	1.53
Main roof	49.8	25.2	6.49	2.42
	49.5	25.4	5.99	2.23
	49.7	24.8	6.18	2.30

TABLE 3

Shear strength test results of coal and rock samples

Lithology	Diameter/mm	Height/mm	Shear angle/(°)	Cohesion/MPa	Internal friction angle/(°)
Coal seam	50.13	50.73	40	11.17	48.23
	50.46	50.65	50		
	50.37	50.31	60		
Immediate roof	50.43	50.87	40	10.72	41.46
	50.26	50.37	50		
	50.64	50.42	60		
Main roof	50.02	50.10	40	9.15	40.23
	50.95	50.50	50		
	50.69	50.97	60		

TABLE 4

Test results of coal and rock firmness coefficient

Impact times	Main roof			Coal seam		
	Data (mm)	Firmness coefficient	Average	Data (mm)	Firmness coefficient	Average
5	13	7.70	7.50	27	3.70	3.80
5	14	7.10		25	4.00	
5	13	7.70		27	3.70	

The test results in Tables 1-4 indicate that the coal seam's average uniaxial compressive and tensile strength values were 23.06 and 0.78 MPa, respectively. The cohesion was 11.17 MPa, the internal friction angle was 48.23°, and the average hardness coefficient was 3.80. While the average uniaxial compressive strength of the main roof rock was 46.36 MPa, the average tensile strength was 2.32 MPa. The cohesion was 9.15 MPa, the internal friction angle was 40.23°, and the average firmness coefficient was 7.50.

3. Analysis of blasting presplitting parameters

3.1. The main influencing factors

Reasonable blasting presplitting parameters (i.e., drilling and blasting ones) control the blasting effect. The drilling parameters mainly include drilling diameter, inclination angle, length, and hole spacing. The blasting parameters are the uncoupling coefficient, linear charge density, charge quantity, hole sealing length, explosive type, cartridge parameters, charging method, and blasting method [14-16]. The details are as follows:

(a) Inclination angle

The blast hole's inclination angle depends on the thickness, length, and direction of the coal seam. An excessive inclination to the goaf side should be avoided. At the same time, the inclination angle of the blast hole also depends on the charging effect. When the blast hole's inclination angle is too large, it is difficult to charge, and the charging quality is difficult to guarantee, which increases the risk of accidental explosion causing casualties. Considering the convenience of charging, the design angle should not exceed 10 degrees. The inclination angle will significantly improve the blasting effect.

(b) Length

In deep-hole loose blasting, the selection of blast hole length is directly related to the mine's production progress and the difficulty of blasting construction. At the same time, reasonable hole depth is also convenient for construction organisation and management. Reasonable hole length can significantly improve the efficiency of blasting operation. The coverage of blasting presplit drilling along the workface inclination should be about half of the workface's length; the fan-shaped drilling layout is more appropriate, and the drilling length should be designed according to the coverage parameters and the main roof position. To ensure the top coal presplitting effect at both ends of the workface, the presplitting drilling should combine long and short holes.

(c) Drilling diameter

In engineering practice, when the drilling hole diameter is too small, in the process of drilling and after drilling, the blast hole is likely to be deformed or bent, which will affect the subsequent charging work. This will narrow the presplitting range of smaller hole diameters, harming the presplitting effect. However, a too large blast hole will increase the workload and difficulty of drilling. It is necessary to comprehensively consider the drilling equipment in the mine, the coal seam's physical and mechanical characteristics, and the available experience in presplitting drilling in similar mines.

(d) Decoupling coefficient

An uncoupled charge is adopted to improve the blasting effect further and make full use of explosion energy. When the charge is uncoupled, the gas generated by blasting expands in the air, which reduces the initial pressure acting on the coal, diminishes the explosive energy consumed by the coal crushing near the charge, and increases the duration of the stress field with the action time of the explosion product pressure. According to the laboratory and field test results, a reasonable uncoupling coefficient is within the range of 1.15 to 1.30, which will be better for improving the blasting effect.

(e) Hole spacing

The distance between blast holes is a key factor controlling the blasting effect. If the distance between blast holes is too large, the presplitting is not sufficient, and it is easy to form large blocks between the two holes; if the distance between blast holes is too small, it will form excessive fragmentation, and the vibration caused by the excess energy of the explosive will also inhibit the support and subsequent mining. Due to the stress concentration between blast holes after blasting, the value of blast hole spacing should be close to the sum of the radii of the fracture zones produced by two adjacent blast holes.

(f) Sealing length

When the cylindrical charge explodes, the coal's antiknock ability increases with the blast hole's depth. The coal breaking ability of the explosive is related to the length of the sealing hole and anti knock strength of the coal. If the sealing hole's depth is too small, the anti-explosion ability will be reduced, thus reducing the blasting effect. If the hole sealing depth exceeds the critical depth, the coal breaking capacity is less than the anti-explosion capacity, and the coal body in the hole sealing section cannot form cracks during the explosion, reducing the blasting effect. According to the field practice and theoretical analysis under similar conditions, the sealing length of deep-hole blasting should be about 1/3 of the hole depth.

(g) Linear charge density and charge quantity

The linear charge density refers to the ratio of blast hole charge quantity to blast hole charge length. Considering the relevant engineering experience and theoretical estimations, the linear charge density is determined as follows:

$$q_1 = \frac{1}{1000} \pi r^2 \frac{\rho_0}{{K_v}^2} \tag{1}$$

where q_1 is linear charge density, kg/m; r is presplit hole radius, mm; ρ_0 *is* explosive density, g/cm; K_v is decoupling coefficient. The charge quantity is the product of the line charge density and charge length.

(h) Initiation mode

The reverse blasting has a higher hole utilisation rate and a better blasting effect, and greater blasting power. There are certain risks when using it in a gas-rich workface, so forward blasting should be preferred. It is necessary to formulate technical safety measures for the reverse initiation.

3.2. Numerical simulation analysis

In this study, three kinds of presplit boreholes were implemented: (i) roof blasting presplit boreholes in workface, (ii) blasting presplitting drilling of coal seam roof in the advanced, and (iii) presplitting drilling of two roadway roof blasting in advance area of the workface. The blasting presplitting drilling mode envisages drilling from the middle to the upper coal seam in the workface. The drilling goes through the top coal and the immediate roof until the main roof is reached. This allows one to realise the synchronous presplitting of the main roof and the top coal. The Yushuling coal mine contained only one type of drilling rig (namely, the ZDY1900S rig), and its drilling diameter was set at 75 mm. Given the single specification of blasting materials in the Xinjiang mine, the optimised blasting parameters and a small-diameter cartridge binding charge were used. Such parameters as inclination angle, length, hole sealing length, drilling, linear charge density, charge quantity, and hole sealing length could be determined via the empirical formulas and comply with the respective mining regulations. Using the above parameters combined with the coal and rock mass properties in the Yushuling coal mine, the effects of borehole spacing and blasting sequence on the blasting presplitting performance were analysed by numerical simulation to determine the most appropriate borehole and blasting parameters.

(a) Material model definition

The ANSYS/LS-DYNA software package contains many mathematical simulation algorithms most applicable to blasting problems, including the Lagrange algorithm and the ALE fluid-structure coupling algorithm [17-20]. The ALE algorithm can overcome the difficulty of numerical calculation caused by a significant distortion of the mesh elements, hence being adopted in this study. A high-explosive material (code 003) was selected and incorporated into the MAT_HIGH_EXPLOSIVE_BURN subprogram, representing the physical and chemical changes in the explosion process. ALE multi-material coupling GROUP is established to connect explosive, air and rock mass, and then fluid-structure coupling is set to connect explosive air Part and rock mass Part. The Jones-Wilkins-Lee equation of state was used to describe the transformation between chemical and internal energies after the explosion. The air was regarded as an ideal gas, and MAT_NULL was selected as a material type. The equation of state is presented by the LINEAR_POLYNOMIAL function. This simulation used the elastic-plastic model, introducing a damage factor based on the Ottosen four-parameter failure criterion, which was realised via the LS-DYNA subprogram called MAT_JOHNSON_HOLMGUIST_CONCRETE. The rock mass material parameters, air, and explosive parameters used in the numerical simulation are summarised in Table 5.

TABLE 5

The blasting presplitting model and equation of state parameters

Material	Parameter	Variable	Value
Emulsion explosive	Density	ρ	1.24 g/cm^3
	Detonation velocity	D	3200 m/s
	CJ pressure	PCJ	2.70 Pa
	JWL parameter 1	A	6.00 MPa
	JWL parameter 2	B	20.09 MPa
	JWL parameter 3	R_1	7.50
	JWL parameter 4	R_2	3.14
	JWL parameter 5	ω	0.08
	Initial specific internal energy	e_0	4.19 Pa
Air	Density	ρ	1.29 kg/m^3
	Initial internal energy	E_0	0.25 Pa
	Equation of state parameters	$C_0 \sim C_3$	0
	Equation of state parameters C1	C_4	0.40
	Equation of state parameters C2	C_5	0.40
	Equation of state parameters C3	C_6	0
	Initial relative volume	V_0	1.00
Rock mass	Density	c	1.29 kg/m^3
	Elastic modulus	E	3.34 GPa
	Poisson's ratio	v	0.374
	Tensile strength	t	2.32 MPa
	Compressive strength	c	46.36 MPa

(b) Numerical model

If the coal and explosives are treated as isotropic and homogeneous materials, the blasting process in the rock mass can be simplified as a plane strain problem, corresponding to the thin shell 163 element type in ANSYS/LS-DYNA [21,22]. Considering the complexity of modelling and calculation of a three-dimensional (3D) numerical model, given the model symmetry and computation efficiency, a rectangular quasi-3D model was elaborated: it had only one unit of thickness, the width of 10 m, and the height of 10 m. The boreholes were arranged on the left and right sides, up and down in the middle. In practice, the blast hole's length significantly exceeds the blast hole diameter so that the edge effect can be ignored, and the initiation point can be set as the centre of the blast hole. In the finite-element model, non-reflective boundary conditions were set at the rock mass boundary, and Z-direction displacement constraints were added. The Lagrange algorithm was selected for the rock mass, and the ALE algorithm was applied to explosives and air to reduce the error caused by large deformation. The ALE-MULTI-MATERIAL-GROUP subprogram was used to link the explosive, air and rock mass, which involved the fluid-solid coupling algorithm [23-25].

(c) Numerical simulation analysis

Four control test groups with blast hole spacing values of 2, 3, 4, and 5 m were set up to study the effect of blast hole spacing on blasting damage of rock mass. The simulation results revealed that the comminution area's fracture area was within a reasonable range at 4 m, and the blasting effect was good. At a blast hole spacing of 4 m, the rock blasting crack expansion was simulated, as shown in Fig. 3.

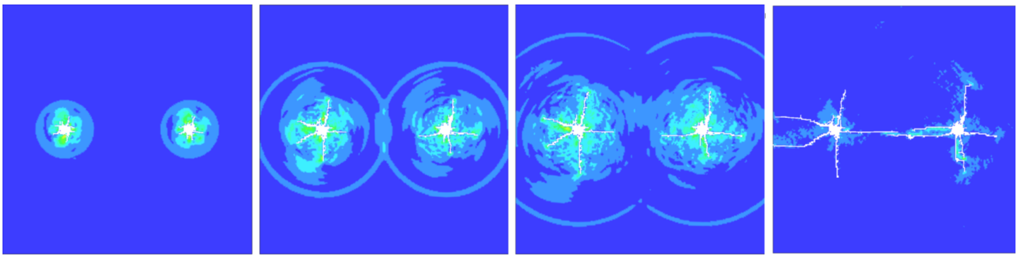

(a) 300 μs, (b) 700 μs, (c) 1000 μs, (d) 4000 μs

Fig. 3. Rock blasting crack expansion with a blast hole spacing of 4 m at different times

As seen in Fig. 3, until 700 μs, the explosions of two blast holes did not influence each other, and the fracture expansion form was similar to the rock damage effect of a single hole explosion. At 300 μs, the comminution zone was formed, and at 700 μs, the effective stress waves of the two holes began to interact. From this point on, the damages of the two holes influenced each other. With the progress of the explosion process at 1000 μs, the large cracks' propagation was almost completed, and the explosion gas and stress action induced the development of fine cracks. At 4000 μs, the damage of the two holes almost reached the maximum, the fracture zone was formed, the damage of rock mass was no longer extended, and the rock between the two blasting holes was fully pre-cracked, reaching the desired range.

To study the blasting damage pattern and its distribution characteristics caused by the blasting sequence, based on determining the blasting distance of 4 m, the explosion in the left blast hole was delayed by 25 ms, as compared to the right blast hole. The rock blasting crack expansion pattern was numerically simulated and depicted in Fig. 4.

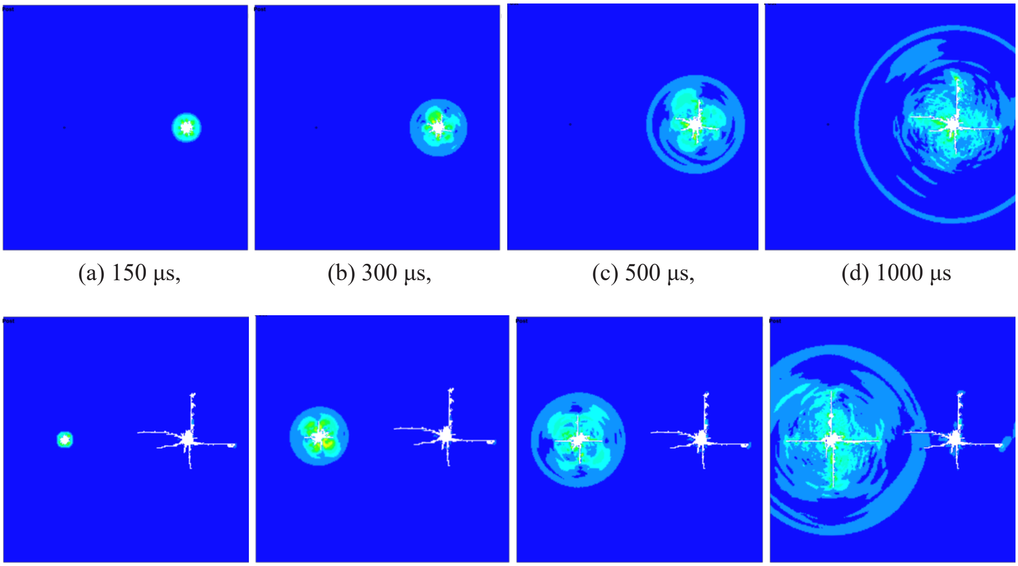

(a) 150 μs, (b) 300 μs, (c) 500 μs, (d) 1000 μs

(a) 25080 μs, (b) 25300 μs, (c) 25500 μs, (d) 26000 μs

Fig. 4. Rock blasting crack expansion of double-hole delayed initiation at different times

As shown in Fig. 4, the explosion damage to the left blast hole was influenced by the explosion loosening of the right one. The fracture area expansion exceeded that of the explosion comminution area. At 25700 μs, i.e., 700 μs after the left blast hole initiation, the left blast stress wave started to interact with the right fracture. Still, due to the distance and time factors, the effect on the left side of the right blast hole was quite weak, leading to a slight expansion of the end fracture near the middle of the right blast hole and not influencing the right side of the right blast hole. As for the left blast hole, at 25700 μs, i.e., 700 μs after the left blast hole initiation, most of the fracture area was formed. Because the rock mass was affected by the explosion of the right blasting hole, the compressive and tensile strength values and the rock integrity deteriorated. The fracture zone formed by the left blasting hole continued to expand after 26000 μs, but the propagation rate was low. In terms of the fracture area's expansion range, the delayed initiation exceeded that of simultaneous initiation. However, although the fracture area of delayed initiation was larger from the rock fragmentation standpoint, that of rock fragmentation was lower than that of simultaneous initiation. Therefore, it was recommended to use the simultaneous initiation scheme.

4. Design of blasting presplitting scheme and effect measurement

4.1. Blasting presplitting drilling layout

4.1.1. Selection of blasting presplitting position

Although the firmness coefficient of top coal in the 110501 workface was high, there were many primary fissures, and the texture was brittle, while the primary fissures of the main roof were not developed. The shallow-buried depth of the 110501 workface was small, and the supporting stress made it difficult to ensure the roof span along with mining. A large area of the hanging roof increased the strata strength of the workface. Therefore, the top coal presplitting borehole's blasting position in the implementation plan was arranged on the main roof of the 110501 workface rather than in its top coal. Through the roof's blasting presplitting, the roof could be respited so that it would collapse with mining to optimise the top coal caving effect and ensure the safe mining of the workface.

4.1.2. Blasting presplitting drilling layout

Three kinds of presplit boreholes were implemented: (i) roof blasting presplit boreholes in the workface, (ii) blasting presplitting drilling of the coal seam roof in the workface's advance area, and (iii) presplitting drilling of two roadway roof blasting in the workface's advance area. The parameters of these three drilling arrangements are listed in Table 6.

TABLE 6

Blasting drilling parameters

Drilling arrangement	**Position**	**Number**	**Length /m**	**Horizon Angle (°)**	**Vertical Angle (°)**
1	**2**	**3**	**4**	**5**	**6**
Roof blasting presplit boreholes in the workface	Workface	1#	14.5	75	75
Blasting presplitting drilling of coal seam roof in the workface's advance area	Transportation roadway	1#	35	30	37
		2#	32	30	30
		3#	30	30	23
		4#	29	30	15
		5#	28	30	8
	Air-return roadway	1#	32	21	42.3
		2#	30.6	23	41.4
		3#	29.5	26	41.4
		4#	28.6	28	41.4
		5#	28.2	30	30.6

TABLE 6. Continued

1	2	3	4	5	6
Presplitting drilling of two roadway roof blasting in the workface's advance area	Transportation roadway	6#	19	6	11.7
		7#	20	4	12.6
		8#	19.5	2	11.7
		9#	20	0	12.6
	Air-return roadway	6#	19	6	11.7
		7#	20	4	12.6
		8#	19.5	2	11.7
		9#	20	0	12.6

(1) Roof blasting presplit boreholes in workface

A row of presplit blasting holes was constructed upward with an angle of 75° between the workface and the coal seam. A hole spacing of 3 m, a hole depth of 14.5m, and a hole diameter of 75 mm were adopted. The actual number of blasting holes was determined according to the workface's length, and all blasting operations were carried out during the workface mining. The layout of presplit boreholes for roof blasting in the workface is shown in Fig. 5.

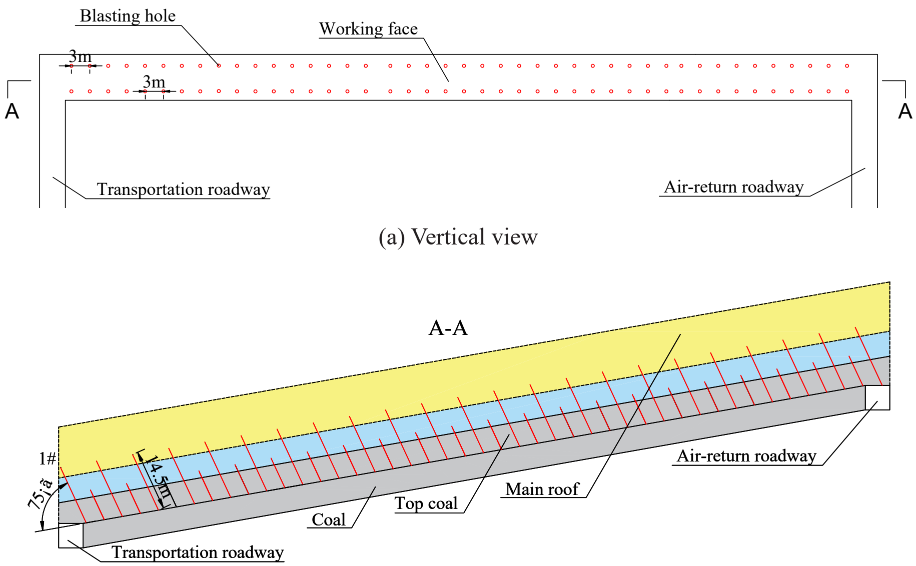

(a) Vertical view

(b) Front view

Fig. 5. Roof blasting presplit boreholes in the workface

(2) Blasting presplitting drilling of coal seam roof in the advance area of the workface

A group of five presplit blasting boreholes was arranged in the transportation and air-return roadways, respectively. Of these, the 1# hole was located 3.9 m away from the coal seam side in the transportation roadway. The holes were arranged in a row on the roadway roof with an interval of 0.3 m, and the blasting was realised when the presplit hole was at 51-80 m from the workface. The layout of presplit boreholes for blasting presplitting drilling of the coal seam roof in the workface's advance area is displayed in Fig. 6.

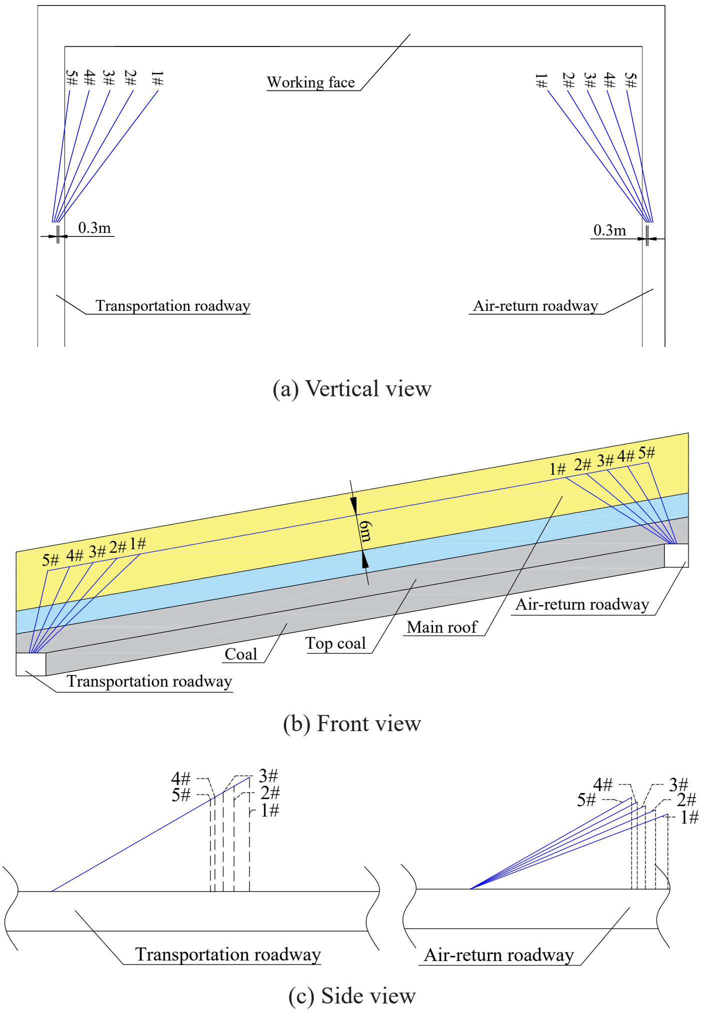

Fig. 6. Blasting presplitting drilling of coal seam roof in the advance area of the workface

(3) Presplitting drilling of two roadway roof blasting in the advance area of the workface

A group of four presplit blasting boreholes was arranged in the transportation and air-return roadway, respectively. The 9# hole was 1.5 m away from the coal pillar side of the air-return roadway, with the holes arranged in a row with an interval of 0.3 m. The blasting was realised when the presplit hole was located at a distance of 55 m from the workface. The respective layout of the presplit boreholes is depicted in Fig. 7.

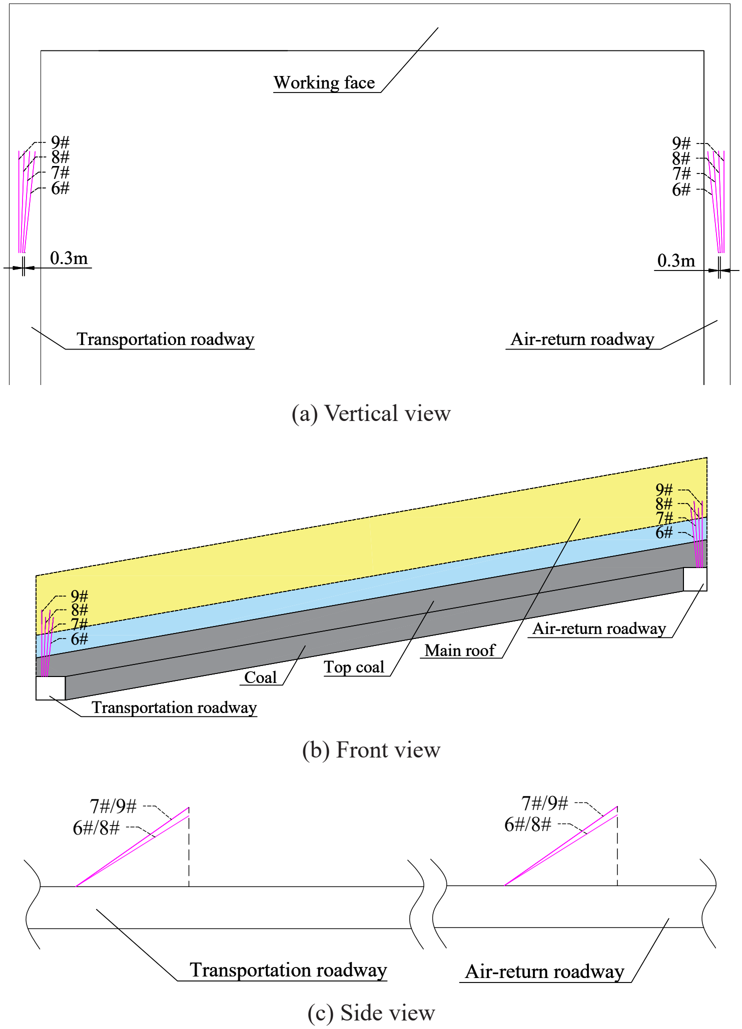

Fig. 7. Presplitting drilling of two roadway roof blasting in advance area of the workface

4.1.3. Charge structure

The charging mode for the three kinds of presplit boreholes was forward charging, with the prompt detonator. The particular charge parameters are shown in Fig. 8 and listed in Table 7.

4.2. Top coal caving effect in the workface

According to the initial mining data, before optimising the top coal presplitting, the top coal recovery rate was low (about 32-41%), with the overall recovery rate below 40%. After implementing the optimisation scheme of the top coal presplitting, the top coal recovery rate

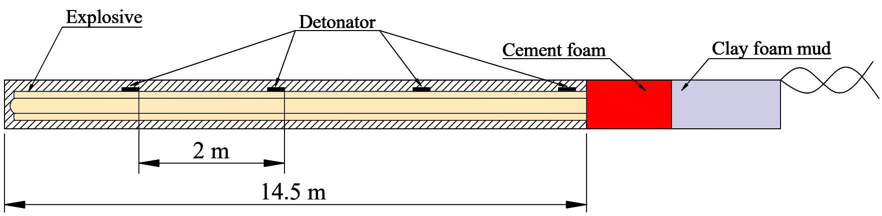

(a) Roof blasting presplit boreholes in the workface

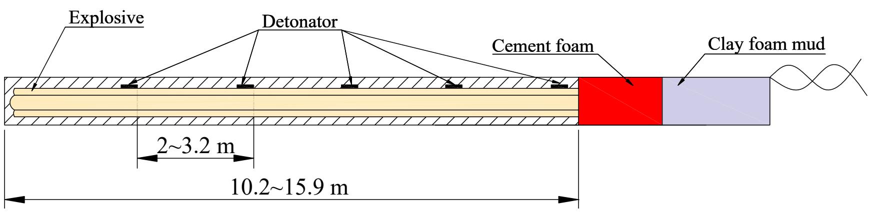

(b) Blasting presplitting drilling of coal seam roof in the advance area of the workface

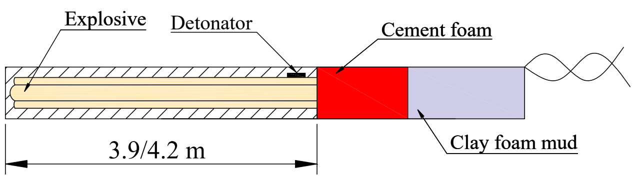

Fig. 8. Charge structure for three kinds of presplit boreholes

TABLE 7

Borehole charge parameters

Position	Drilling hole	Length /m	Charge length /m	Primary explosive roll /piece	Charge mass /kg
1	2	3	4	5	6
Workface	1#	14.5	6.7	1	20
Transportation roadway	1#	35	15.9	5	47.7
	2#	32	14.1	5	42.3
	3#	30	12.6	5	37.8
	4#	29	12.3	5	36.9
	5#	28	10.2	5	30.6
Air-return roadway	1#	32	14.1	5	42.3
	2#	30.6	13.8	5	41.4
	3#	29.5	13.8	5	41.4
	4#	28.6	13.8	5	41.4
	5#	28.2	10.2	5	30.6
Transportation roadway	6#	19	3.9	1	11.7
	7#	20	4.2	1	12.6
	8#	19.5	3.9	1	11.7
	9#	20	4.2	1	12.6

TABLE 7. Continued

1	2	3	4	5	6
Air-return roadway	6#	19	3.9	1	11.7
	7#	20	4.2	1	12.6
	8#	19.5	3.9	1	11.7
	9#	20	4.2	1	12.6

was significantly improved (with the average value of 80.5%), reaching its maximum of 87% on Day 3 (namely, August 22, 2020), the daily advance through the blast holes is at the same level. The caving effect of the method was excellent, and the workface's recovery rates after presplitting optimisation were listed in Table 5. Field photos of presplit drilling in transportation and air-return roadways were shown in Fig. 9, and those in the goaf were displayed in Fig. 10.

TABLE 8

The coal recovery rate of the workface after optimis ation of the top coal presplitting parameters

Day	Daily advance /m	Mining position /m	Thickness /m	Workface length /m	Reserves /t	Production /t	Recovery rate /%
1	3.2	329.4	8.6	155	4997	4151.83	83
2	3.2	332.6			4997	4148.79	83
3	3.2	335.8			4997	4340.17	87
4	3.2	339			4997	4121.74	82
5	3.2	342.2			4997	4210.83	84
6	3.2	345.4			4997	3658.00	73
7	3.2	348.6			4997	3883.61	78

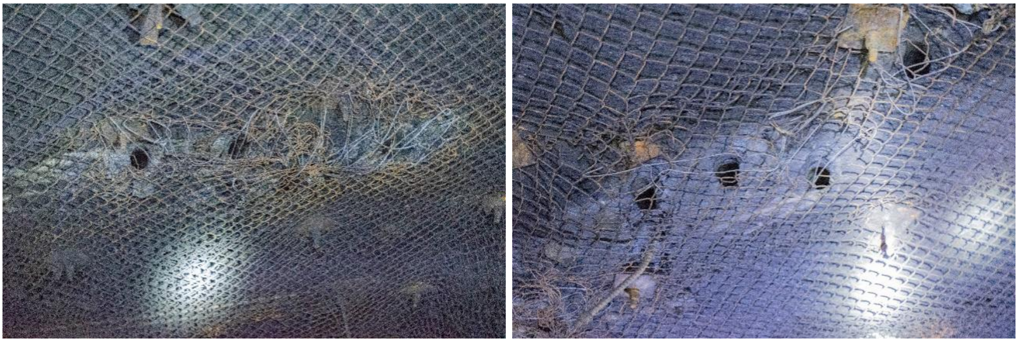

Fig. 9. Field photos of presplit drilling in transportation and air-return roadways

As seen in Fig. 10, the caving effect of the top coal behind the support was good, and the caving coal block was moderate. The roof of about 2 m in the goaf was also fully caving, and its block size was generally larger than that of the top coal, so it was difficult to enter the coal drawing mouth, which could ensure a lower gangue rate. The above blasting drilling design method has achieved a sufficient field application effect.

Fig. 10. Field photos of presplit drilling in the goaf

The average coal thickness of 110501 fully mechanised top coal caving face is 8.6 m, the average mining height is 4.0 m, and the mining caving ratio is 1:1.15. By adopting the presplitting blasting method, a total of 1176600 tons of coal had been recovered from April 2020 to March 2021, and the maximum daily coal output reached 5858.21 tons, which achieved satisfactory engineering results. The mining condition of 110501 fully mechanised top coal caving face is shown in Fig. 11.

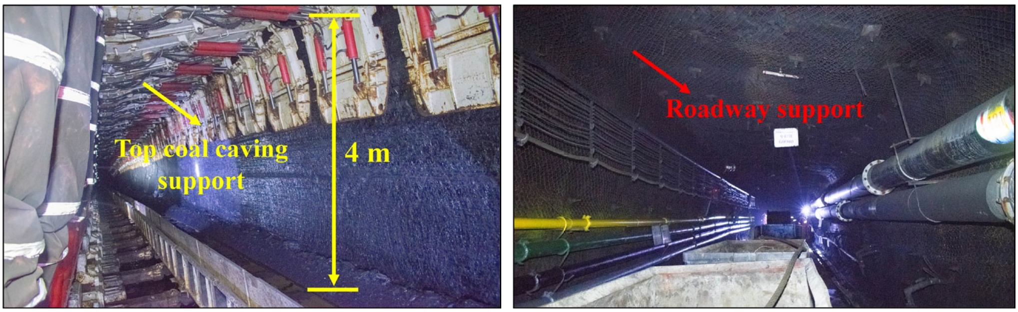

Fig. 11. Field application photos of 110501 working face

5. Conclusions

(1) Physical properties and mechanical characteristics of the coal and rock mass in the Yushuling coal mine included the coal seam's average uniaxial compressive and tensile strength values of 23.06 and 0.78 MPa, respectively. The cohesion, internal friction angle, and average firmness coefficient were 11.17 MPa, 48.23°, and 3.80, respectively. The main roof rock had the average uniaxial compressive and tensile strength values of 46.36 and 2.32 MPa, a cohesion of 9.15 MPa, an internal friction angle of 40.23°, and an average firmness coefficient of 7.50.

(2) The effect of different factors on the blasting presplitting effect was numerically simulated, using reasonable blasting drilling parameters. The drilling diameter was set

at 75 mm, the borehole spacing was about 4 m, and a small-diameter cartridge binding charge was adopted. The blasting presplitting drilling mode envisaged drilling from the middle to the upper coal seam in the workface. The drilling went through the top coal and the immediate roof until the main roof was reached to realise the synchronous presplitting of the main roof and top coal. Three kinds of presplit boreholes were implemented; namely, roof blasting presplit boreholes in the workface, the workface's advance area, and two roadway roofs. The optimal blasting drilling parameters and charge structure were identified.

(3) The field test results show that the top coal recovery rate of the 110501 FMTC caving face was increased more than twice (from 40 to more than 80%), and a remarkable blasting presplitting effect was achieved. Regarding the restrictions on the use of explosives in coal mines of Xinjiang Province (natural hazards, safety factors, regional restrictions etc.). This blasting presplitting method has important guiding significance for the FMTC caving mining in Xinjiang and similar mining areas.

Author Contributions

Qiang Sun proposed and verified the innovative method; Yunbo Wang established and implemented the numerical and physical models; Zhongya Wu analys ed the data; Qiang Sun wrote the paper; Chengfang Shan and Qiang Sun revised the paper.

Funding

The authors appreciate the financial support of this work provided by the China Postdoctoral Science Foundation (grant No.2020M671650).

Acknowledgments

The authors would like to thank the editors and reviewers for their comments and professional suggestions that helped to improve this paper's quality.

Reference

[1] G.R. Feng, Y.J. Zhang, T.Y. Qi, L.X. Kang, Status and research progress for residual coal mining in China. J. China. Coal. Soc. **45** (01), 151-159 (2020).

[2] J. Wang, F. Liu, J. Zhang, Investigation on the propagation mechanism of explosion stress wave in underground mining. Geomech. Eng. **17** (3), 297-307 (2019).

[3] Z.F. Bian, S.G. Lei, Green exploitation of coal resources and its environmental effects and protecting strategy in Xinjiang. Int. J. Coal. Sci. Technol. **48** (04), 43-51 (2020).

[4] D.S. Zhang, H.L. Liu, G.W. Fan, X.F. Wang, Connotation and prospection on scientific mining of large Xinjiang coal base. J. Min. Safety. Eng. **32** (01), 1-6 (2015).

[5] Y.F. Feng, Research on weakening technology of hard dirt band presplitting blasting based on LS-DYNA. Chinese. J. Under. Space. Eng. **12** (S2), 726-732 (2016).

[6] B. Yu, H.F. Duan, Study of roof control by hydraulic fracturing in full-mechanized caving mining with high strength in extra-thick coal layer. Chinese. J. Rock. Mech. Eng. **33** (4), 778-778 (2014).

[7] T. Berard, J. Desroches, Geological structure, geomechanical perturbations, and variability in hydraulic fracturing performance at the scale of a square mile. Geomech. Energy. Envir. **26**, 100137 (2019).

[8] D.M. Zhang, X. Bai, G.Z. Yin, Z. Rao, Q.B. He, Research and application on technology of increased permeability by liquid CO_2 phase change directional jet fracturing in low-permeability coal seam. J. China. Coal. Soc. **43** (7), 1938-1950 (2018).

[9] D. Mondal, P.N.S. Roy, Fractal and seismic b-value study during dynamic roof displacements roof fall and surface blasting) for enhancing safety in the longwall coal mines. Eng. Geol. **253**, 184-204 (2019).

[10] Y. Jiang, R. Misa, K. Tajdus, A. Sroka, Y. Jiang, A new prediction model of surface subsidence with cauchy distribution in the coal mine of thick topsoil condition. Arch. Min. Sci. **65** (1), 147-158 (2020).

[11] T. Janoszek, The assessment of longwall working stability based on the mohr-coulomb stress criterion-numerical analysis. Arch. Min. Sci. **65** (3), 493-509 (2020).

[12] R.S Yang, Y. Zhu, Y.L. Li, W.Y. Li. Coal ribs stability analysis and control countermeasures of bare roof roadway under hard roof condition. J. Min. Safety. Eng. **37** (5), 861-870 (2020).

[13] M.C. He, Y. Yuan, X.L. Wang, Z.Q. Wu, Q. Zhao, C. Liu, Y.L. Jiang. Control technology for large deformation of Mesozoic compound soft rock in Xinjiang and its application. Chinese. J. Rock. Mech. Eng. **32** (3), 433-441 (2013).

[14] J. Liu, Z.G. Liu, K. Gao, J.H. Xue, Y.B. Lou, Experimental study of extension characters of cracks in coal seam under blasting load with different charging modes. Chinese. J. Rock. Mech. Eng. **35** (4), 735-742 (2016).

[15] F. Liu, J. Silva, S. Yang, H. Lv, J. Zhang, Influence of explosives distribution on coal fragmentation in top-coal caving mining. Geomech. Eng. **18** (2), 111-119 (2019).

[16] Y. Luo, K. Xu, J.H. Huang, X.P. Li, T.T. Liu, D.X. Qu, P.P. Chen, Impact analysis of pressure-relief blasting on roadway stability in a deep mining area under high stress. Tunn. Under. Sp. Tech. **110**, 103781 (2021).

[17] B. Liang, L.F. Jia, W.J. Sun, Z.S. Shi, H. Zhao, Q. Dong, Experimental study of mechanical properties for grouted sealing material in deep hole pre-splitting blasting. Exp. Mech. **32** (1), 123-130 (2017).

[18] M.C. He, P.F. Guo, X.H. Zhang, J. Wang, Directional pre-splitting of roadway roof based on the theory of bilateral cumulative tensile explosion. Combust. Explo. Shock. Waves. **38** (4), 795-803 (2018).

[19] Q.L. Liu, X.F. Meng, X.C. Li, X.X. Luo, Risk precontrol continuum and risk gradient control in underground coal mining. Process. Saf. Environ. **129**, 210-219 (2019).

[20] G.F. Wang, F. Liu, Y.H. Pang, H.W. Ren, Y. Ma, Coal mine intellectualization: The core technology of high-quality development. J. China. Coal. Soc. **44** (02), 5-13 (2019).

[21] S.J. Qu, J.F. Liu, Numerical analysis of joint angle effect on cracking with presplit blasting. Rock. Soil. Mech. **36** (1), 189-194 (2015).

[22] Y. Sen, Fatigue fracture analysis of the semi-auto shotgun mechanism by using finite element analysis and experimental setup. Eng. Fail. Anal. **11 7**(20), 104963 (2020).

[23] T.H. Xu, L.M. Zhang, Numerical implementation of a bounding surface plasticity model for sand under high strain-rate loadings in LS-DYNA. Comput. Geotech. **66**, 203-218 (2015).

[24] R.F. Liu, Z.M. Zhu, Y.X. Li, B. Liu, D.Y. Wang, M. Li, Study of rock dynamic fracture toughness and crack propagation parameters of four brittle materials under blasting. Eng. Fract. Mech. **225**, 106460 (2019).

[25] H. Ma, J. Chen, D. Wang, S. Su, X. Yang, Simulation and experimentation of torkbuster based on ANSYS/LS-DYNA. Int. J. Oil. Gas. Coal. Technol. **6** (4), 50 (2018).